Journal of Energy Storage 97 (2024) 112941

Contents lists available at ScienceDirect

Journal of Energy Storage

journal homepage: www.elsevier.com/locate/est

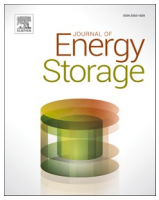

Research papers

A case study of optimising energy storage dispatch: Convex optimisation approach with degradation considerations

Jonas Vaičys [a,*], Saulius Gudžius [a], Audrius Jonaitis [a], Roma Račkienė [a], Andrei Blinov [b], Dimosthenis Peftitsis [c]

[a] Department of Electrical Power Systems, Kaunas University of Technology, Lithuania
[b] Department of Electrical Power Engineering and Mechatronics, Tallinn University of Technology, Estonia
[c] Department of Electrical Power Engineering, Norwegian University of Science and Technology, NO-7491 Trondheim, Norway

ARTICLE INFO

Keywords:
Battery energy storage degradation
Renewable energy storage
Hybrid renewable energy system
Day-ahead dispatch
Convex optimisation

ABSTRACT

The integration of renewable energy sources (RES) like solar photovoltaics (PV) into power grids is crucial for global sustainability goals. As RES integration accelerates, energy storage systems, particularly electro-chemical battery energy storage systems (BESS), become vital to address supply-demand gaps. This paper focuses on the optimisation of day-ahead BESS operation dispatch in hybrid renewable energy systems (HRES) using convex optimisation technique which ensures distinct charging and discharging states of BESS. Since this novel approach involves BESS degradation into decision making process, it enables to dispatch the whole HRES by using BESS lifecycle more efficiently and it also leads to a more accurate estimation of HRES economic feasibility. Our proposed method is benchmarked with naive, self-consumption, mixed integer linear programming (MILP) and linear programming (LP) models by using real data of HRES installed in Kaunas University of Technology, Lithuania. The results of this case study showed that application of convex non-linear model allowed partial BESS cycling, unlike other analysed methods. Consequently, BESS performed 2.36 times more cycles per year, which led to increased IRR by up to 10 % compared to commonly used MILP and LP models. These outcomes underline the importance of the development of new BESS dispatch optimisation strategies that lead to holistic approach in overall HRES payback evaluation.

1. Introduction

The increasing integration of renewable energy sources (RES), such as solar photovoltaics (PV), into power grids represents a pivotal global transition toward sustainable and low-carbon energy systems [1]. This shift aligns with the European Union [2] and United Nations [3] sustainable development goals, emphasizing the need to address climate change, ensure affordable and clean energy, and promote responsible consumption and production. Under the International Renewable Energy Agency (IRENA) 1.5 °C Scenario [4] would require a cumulative global installed renewable electricity generation capacity of over 11 174 GW of which 5457 GW is planned to receive from solar PV. However, as the integration of RES into power grids accelerates globally, challenges emerge in aligning these ambitions with practical implementation, necessitating crucial investments into energy storage systems [5].

Energy storage plays a fundamental role in mitigating shortfalls between the supply and demand of electricity generated from RES [6]. Various energy storage [7], including electrical [8], thermal [9], electro-chemical [10], chemical (including hydrogen), hydro pumped [11] and mechanical storage [12], contribute to ensuring the stability and reliability of the grid [13]. Among these technologies, battery energy storage systems (BESS), particularly electro-chemical BESS, stands out as a major component for the integration of RES [6,7,10].

Electro-chemical BESS [10] are classified into types such as lithium-ion, lead-acid, or nickel batteries, zinc bromine flow batteries, and metal-air batteries [7,9]. Additionally, technologies like flow batteries, supercapacitors, and superconducting magnetic energy storage also fall under the category of electro-chemical BESS [8,9]. All these types [14] can effectively store the generated electricity from RES [15,16]. Furthermore, due to their rapid response [17], flexible installation, and short construction cycles [18], they are among the most widely adopted energy storage technologies in electric power systems [10,19,20].

Different battery energy storage [16] technologies are utilized on a commercial scale, chosen based on application-specific characteristics

* Corresponding author.
E-mail address: jonas.vaicys@ktu.lt (J. Vaičys).

https://doi.org/10.1016/j.est.2024.112941
Received 10 January 2024; Received in revised form 19 June 2024; Accepted 8 July 2024
Available online 1 August 2024

Nomenclature

c_e	Energy spot price (Eur/MWh)
ε	Fixed grid usage charge for consumption (Eur/MWh)
p_L	Total load (consumption) (kW)
p_{pv}	Generated solar PV power (kW)
p_{cu}	Curtailed solar PV power (kW)
p_{buy}	Power bought from the market (kW)
p_{sell}	Power sold to the market (kW)
p_{ch}	Power used for charging BESS (kW)
p_{dch}	Power discharged from BESS discharged (kW)
η_{ch}	BESS charging efficiency (decimal %)
η_{dch}	BESS discharging efficiency (decimal %)
SOC	State of Charge (kWh)

like charge-discharge rates, energy storage capacity, power, and response time. One prominent technology is lithium-ion (Li-ion) [21] batteries, functioning through the movement of lithium ions between positive and negative electrodes during charging and discharging [22]. Li-ion batteries are characterized by high efficiency (almost 99 % [23]), low self-discharge rate (2–8 % per month [24]), a long cycle life (higher than 1000 cycles [25]), and wide operating temperature range (Li-ion batteries may charge between 0 and 45 °C and discharge between −40 and 65 °C [26,27]).

Since the capital costs of Li-ion batteries in power systems fall within the range 200 to 500 Eur/kWh [28], the economic planning of such BESS integration in hybrid renewable energy systems (HRES) is an ongoing area of research and testing [29–31]. Li-ion based batteries, with their higher life cycle and efficiency compared to the most popular Lead-acid batteries, offer a preferable choice for HRES [32], especially the ones, which include photovoltaic panels and aim to efficiently store and utilize solar power [32,33].

There are two main types of HRES applications, namely, off-grid and grid-connected HRES [34–36]. Many researchers [37–43] have worked on the comparison between these systems in economic, technical, environmental, and other aspects. Their results claim that while off-grid systems offer complete energy independence, their limited capacity and high battery costs make them suitable for sparsely populated remote areas [41,42]. In contrast, grid-connected HRES ensure uninterrupted energy supply by storing excess energy from RES and supplying it to the grid when needed, including black-outs [37,39]. Therefore, for enhanced energy stability, it is more beneficial to implement grid-connected systems [38].

To increase the overall efficiency of HRES, optimisation techniques are applied to both off-grid and grid-connected systems [40,43]. The key focus of HRES design is BESS [44–46] as it provides such advantages, as energy reliability by offering a buffer during periods when the renewable sources are not generating power [47,48], grid stability by helping in peak cutting and load leveling [49,50] and optimised use of resources by intelligently managing the energy storage to maximize the efficiency of different energy resources [51].

Authors [52] raise the frequency related issues posed by the increasing penetration level of RES. A study conducted in Texas highlights the increasing importance of grid-scale energy storage in meeting flexibility and system inertia needs [53]. Another compelling example showcasing the significance of day-ahead optimisation is the BESS directly dispatched by grid operators to effectively provide active power regulation services, such as, inertia frequency response, frequency containment reserve, frequency restoration reserve, and peak regulation, to contribute to economic benefits and enhanced grid reliability [54]. Utilization of dynamic pricing optimisation in BESS operation dispatch can also increase its versatility in minimizing operating costs and maximizing benefits across applications like peak shifting, Demand Response, and Time of Use [55].

The optimisation of the BESS design and operation dispatch is to improve the matching of the battery capacity and charging/discharging profiles with energy demands [56]. During charging, the energy storage battery must receive a constant and adequate charging current. Undercharging or overcharging can damage the battery [57] and reduce energy efficiency. During discharge, the system must avoid sudden power spikes and drops and transfer the stored energy to the grid or the user in a smooth and controlled manner. Discharge and charge management with appropriate power management systems maintain efficiency and extend battery life [58,59]. Battery cells may degrade over time and therefore have a lower capacity than originally purchased.

As the optimisation of day-ahead BESS operation dispatch [55] introduces intertemporal time constraints for charging and discharging decisions at specific periods, addressing the challenge of non-simultaneous charging and discharging becomes crucial [60]. To tackle this, various authors employ nonlinear models, such as Mixed Integer Linear Programming (MILP) [61–63]. However, using binary variables introduces non-convexity, leading to less efficient solvers [64]. This non-convex nature can significantly escalate computational challenges, particularly in large-scale optimisation problems or when optimising local controllers [65]. The computational burden associated with non-convex formulations underscores the importance of exploring alternative approaches that balance accuracy and computational efficiency in practical implementation of optimisation techniques [66].

In this regard, [64] proposes a convex formulation of the problem by incorporating penalty-based relaxation to discourage non-simultaneousness. Authors [67,68] also highlight sufficient conditions under which the penalty-based approach ensures non-simultaneousness. The objective of this research is to enhance the precision and efficiency of these existing models for the day-ahead operation dispatch of BESS by incorporating its degradation costs. For this purpose, we propose a more detailed nonlinear approach falling under the umbrella of convex optimisation.

In this context, as BESS becomes essential for grid stability and the economic feasibility of HRES, it is crucial to develop optimisation strategies that account for BESS degradation over its lifecycle. This research introduces a convex nonlinear programming (NLP) model that ensures distinct charging and discharging states while promoting partial cycling of BESS, reducing degradation, and extending operational life. Our model is benchmarked against naive, self-consumption, MILP, and LP models using real data from an HRES at Kaunas University of Technology, Lithuania. The results show that our model significantly increases BESS cycles and the internal rate of return, underscoring the importance of considering BESS degradation in optimisation for more accurate economic feasibility assessments.

To demonstrate the economic benefits of our proposed method, this paper is organized as follows: Section 2 introduces the mathematical challenges related to day-ahead BESS operation dispatch optimisation and degradation modeling. Following that, Section 3 presents the methodology for developing test scenarios from validated real data and their subsequent evaluation. Section 4 provides comprehensive case study results, benchmarking our proposed model against naive and baseline models, along with a sensitivity analysis. Finally, Section 5 offers conclusions based on the findings presented.

2. Mathematical models of HRES operation dispatch optimisation

The optimisation of day-ahead dispatch poses a mathematical challenge due to intertemporal time constraints arising from a sequential multistep decision-making process. Specifically, the BESS operation involves charging and discharging decisions at specific time periods, influencing subsequent states and available capacities. To address this challenge, the mathematical formulation of the problem must explicitly consider the time-varying constraints related to SOC evolution.

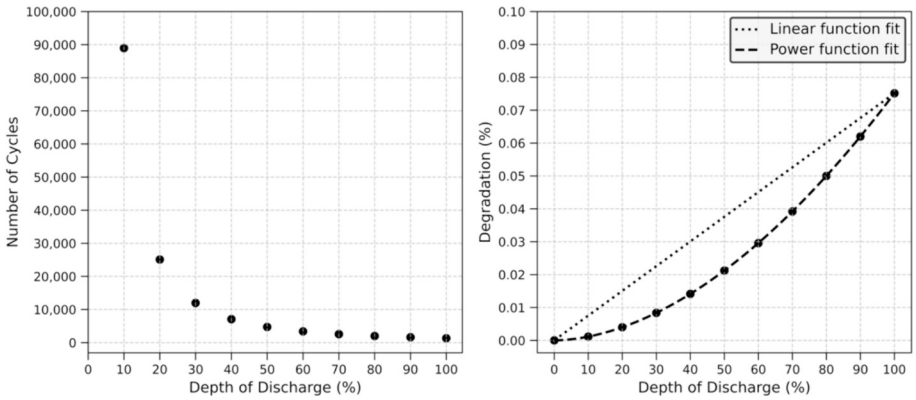

Fig. 1. Li-ion BESS number of cycles (a) and corresponding degradation (b) (based on [72]).

The bidirectional power flow nature of energy storage makes the day-ahead dispatch optimisation problem non-convex. To prevent simultaneous charging and discharging, a common approach is to use binary variables, transforming the problem into a MILP. As suggested by [61–63], the constraints of such BESS dispatch optimisation problem can be expressed as in Eqs. (1a)–(1e).

$$SOC^{(t+1)} = SOC^{(t)} + \Delta t\left[\eta_{ch}p_{ch}^{(t)}b^{(t)} - \eta_{dch}p_{dch}^{(t)}\left(1-b^{(t)}\right)\right] \tag{1a}$$

$$\underline{SOC} \le SOC^{(t)} \le \overline{SOC} \tag{1b}$$

$$0 \le p_{ch}^{(t)} \le \overline{p_{ch}} \tag{1c}$$

$$0 \le p_{dch}^{(t)} \le \overline{p_{dch}} \tag{1d}$$

$$b^{(t)} \in \{0,1\} \tag{1e}$$

for all time $t \in \{1,\ldots,N\}$. Hereinafter, the underscore and bar denote the minimum and maximum allowed values of variables, which are described in the Nomenclature section.

As detailed in [69], to solve a problem containing binary variable(s), typically commercial solvers that implement Branch and Bound methods or alternative methods are used. However, contrary to the traditional MILP approach, convex optimisation techniques can offer advantages through more efficient solutions without the need for discrete variables and large combinatorial considerations. A generic structure for a convex optimisation problem is expressed as in Eqs. (2a)–(2c):

$$min f_0(x) \tag{2a}$$

subject to:

$$f_i(x) \le b_i, i = 1,\ldots,m \tag{2b}$$

$$f_i(\alpha x + \beta y) \le \alpha f_i(x) + \beta f_i(y), i = 1,\ldots,m \tag{2c}$$

for all $x, y \in \mathbb{R}^n$ and all $\alpha, \beta \in \mathbb{R}$ with $\alpha + \beta = 1$, $\alpha \ge 1$, $\beta \ge 1$.

Authors in [60] analyse and conclude that using a convex approach for BESS dispatch optimisation problem requires to penalize charging and discharging in objective function using parameters α and β as described in Eqs. (3a)–(3e). These parameters are specifically used to prevent from simultaneous charging and discharging, which can occur in HRES when generation exceeds consumption.

$$\min_{P_{ch},P_{dch}} \Delta t\sum_{t=1}^{N}\left[\left(p_{ch}^{(t)} - p_{dch}^{(t)}\right)c_e^{(t)} + \alpha p_{ch}^{(t)} + \beta p_{dch}^{(t)}\right] \tag{3a}$$

subject to:

$$\underline{SOC} \le SOC^{(0)} - \Delta t\sum_{n=1}^{t}\left(\eta_{dch}p_{dch}^{(t)} - \eta_{ch}p_{ch}^{(t)}\right) \tag{3b}$$

$$SOC^{(0)} + \Delta t\sum_{n=1}^{t}\left(\eta_{ch}p_{ch}^{(t)} - \eta_{dch}p_{dch}^{(t)}\right) \le \overline{SOC} \tag{3c}$$

$$0 \le p_{ch}^{(t)} \le \overline{p_{ch}} \tag{3d}$$

$$0 \le p_{dch}^{(t)} \le \overline{p_{dch}} \tag{3e}$$

for all time $t \in \{1,\ldots,N\}$. These penalization parameters can in fact be used to model BESS degradation phenomenon, which shall not be neglected [70,71]. Such transformation turns the optimisation problem into a trade-off between the economic benefits of energy spot price spreads and the associated degradation costs by allowing not only full but also partial cycling of BESS.

2.1. BESS degradation modeling

Integrating BESS degradation into the day-ahead dispatch optimisation problem is crucial for assessing the impact of cycling on the BESS lifetime. BESS lifetime is limited by the cumulative number of charge-discharge cycles it undergoes, and this is linked to the DoD by non-linear relationship. Although there is a variety of existing and emerging energy storage technologies which possess different degradation characteristics, our analysis focuses on, but is not limited to, one of the most mature technologies as of the time of writing – the Li-ion battery.

Fig. 1 illustrates the number of cycles and degradation (δ) at various DoD levels of a typical Li-ion battery. To quantify this degradation behaviour, two distinct fit functions are employed, namely, linear Eq. (4a) and non-linear Eq. (4b).

$$\delta = k{\cdot}DoD \tag{4a}$$

$$\delta = a{\cdot}DoD^b \tag{4b}$$

The linear fit function with a slope $k = 0.075$ is chosen for its simplicity and efficiency in the context of MILP and LP methods. These methods benefit from the linear relationship between the degradation and DoD, enabling straightforward integration into the optimisation models. However, it is important to note that the linear fit function is more conservative than the power fit function. In optimisation models where the linear fit function is implemented, BESS operation will be more constrained compared to the case with the NLP model, which utilizes the power fit function. This observation implies that LP models are likely to exhibit lower levels of degradation and, consequently, slower BESS payoff and lower HRES savings.

The power fit function, coefficients of which are $a = 1.68 \bullet 10^{-5}$ and $b = 1.825$ by [72], characterized by its non-linear nature, is selected for

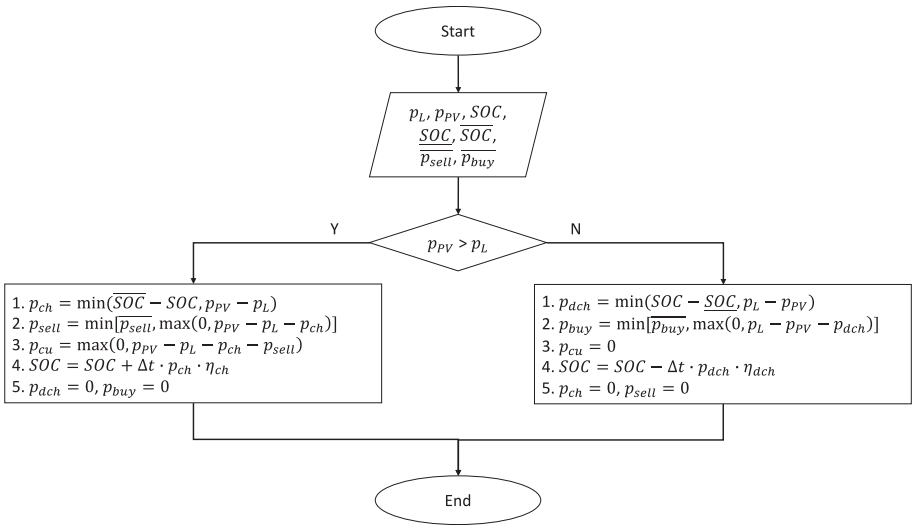

Fig. 2. Naive (Self-consumption) model algorithm flowchart.

the proposed NLP model. The non-linear relationship between the degradation and DoD is better captured by this function, making it suitable for optimisation methods that can handle non-linear constraints.

These fitted functions, tailored to the degradation characteristics of Li-ion batteries, play a crucial role in developing optimisation models. The choice of linear or power fit functions is driven by the specific requirements and capabilities of the optimisation methods employed in this study.

2.2. Mathematical formulation of different optimisation approaches

In this section, four distinct models are formulated: Naive (Self-consumption) model, Baseline (MILP) model, Convex (LP), and our proposed Convex (NLP) model.

2.2.1. Naive model

The Naive model, also known as Self-consumption mode [73], involves no day-ahead dispatch optimisation. Mathematically, it is represented for each time step as shown in Fig. 2. The primary objective in self-consumption mode is to maximize the utilization of locally generated renewable energy. This is achieved by storing surplus energy in the BESS during periods of excess generation and utilizing it when renewable energy falls short of on-site demand, thereby enhancing the sustainability of the energy system, irrespective of energy spot prices. The Naive model is included for comparison reasons to illustrate the general purpose and impact of different optimisation methods applied in this paper.

2.2.2. Baseline (MILP) model

The MILP model is widely adopted in various research articles [61–63]. It utilizes a binary variable, as detailed in Eqs. (5a)–(5j), to prevent simultaneous charging and discharging. Hence, it is designated as the baseline model, serving as the benchmark. The objective function of the Baseline model is designed to minimize the total HRES cost over the days' time span, which includes the linear fit function of BESS degradation costs.

$$\min_{p_{ch},p_{dch},p_{buy},p_{sell},p_{cu},b} \Delta t \sum_{t=1}^{N} \left[p_{buy}^{(t)} \left(c_e^{(t)} + \varepsilon \right) - p_{sell}^{(t)} c_e^{(t)} + \gamma \left(p_{ch}^{(t)} + p_{dch}^{(t)} \right) \right] \tag{5a}$$

subject to:

$$p_L^{(t)} - p_{buy}^{(t)} + p_{sell}^{(t)} + p_{ch}^{(t)} b^{(t)} - p_{dch}^{(t)} \left(1 - b^{(t)} \right) - p_{PV}^{(t)} + p_{cu}^{(t)} = 0 \tag{5b}$$

$$SOC^{(t+1)} = SOC^{(t)} + \Delta t \left[\eta_{ch} p_{ch}^{(t)} b^{(t)} - \eta_{dch} p_{dch}^{(t)} \left(1 - b^{(t)} \right) \right] \tag{5c}$$

$$\underline{SOC} \leq SOC^{(t)} \leq \overline{SOC} \tag{5d}$$

$$0 \leq p_{ch}^{(t)} \leq \overline{p_{ch}} \tag{5e}$$

$$0 \leq p_{dch}^{(t)} \leq \overline{p_{dch}} \tag{5f}$$

$$0 \leq p_{buy}^{(t)} \leq \overline{p_{buy}} \tag{5g}$$

$$0 \leq p_{sell}^{(t)} \leq \overline{p_{sell}} \tag{5h}$$

$$0 \leq p_{cu}^{(t)} \leq \overline{p_{PV}^{(t)}} \tag{5i}$$

$$b^{(t)} \in \{0, 1\} \tag{5j}$$

For all time $t \in \{1, \ldots, N\}$. Here, ε denotes the fixed grid usage charge for consumption [Eur/MWh], which is normally higher for consumers at low voltage levels compared consumers connected to medium and high voltage levels. Also, γ here is expressed as $\gamma = \frac{k_\xi}{2}$ in [Eur/MWh], where ξ denotes energy cells refurbishment costs related to degradation through cycling [Eur/MWh].

The Baseline model without degradation considerations (Baseline-NOD) maintains the same structure as the Baseline model, with the sole modification in the objective function, as indicated in Eq. (6). This variant is included for comparative analysis, demonstrating that neglecting costs associated with BESS degradation leads to a lower overall economic benefit. Validation for this model is omitted as it represents a simplified version of the Baseline model.

$$\min_{p_{ch},p_{dch},p_{buy},p_{sell},p_{cu},b} \Delta t \sum_{t=1}^{N} \left[p_{buy}^{(t)} \left(c_e^{(t)} + \varepsilon \right) - p_{sell}^{(t)} c_e^{(t)} \right] \tag{6}$$

2.2.3. Convex model (LP)

A convex model (LP) that guarantees non-simultaneous charging and discharging is similar to MILP model, except it does not have binary variable in power balance equation Eq. (7b) and Eqs. (5c), (5d) are replaced by Eqs. (7c), (7d) to enforce the SOC limit constraints. This model is included to validate and showcase that convex approach can be used to achieve the same BESS operation dispatch results as using MILP

method. This is particularly important step, because convex optimisation, in general, can deal with convex functions which can be non-linear, for example, the power fit function of BESS degradation and DoD.

$$\min_{p_{ch},p_{dch},p_{buy},p_{sell},p_{cu}} \Delta t \sum_{t=1}^{N} \left[p_{buy}^{(t)} \left(c_e^{(t)} + \varepsilon \right) - p_{sell}^{(t)} c_e^{(t)} + \gamma \left(p_{ch}^{(t)} + p_{dch}^{(t)} \right) \right] \tag{7a}$$

subject to:

$$p_L^{(t)} - p_{buy}^{(t)} + p_{sell}^{(t)} + p_{ch}^{(t)} - p_{dch}^{(t)} - p_{PV}^{(t)} + p_{cu}^{(t)} = 0 \tag{7b}$$

$$\underline{SOC} \leq SOC^{(0)} - \Delta t \sum_{n=1}^{t} \left(\eta_{dch} p_{dch}^{(t)} - \eta_{ch} p_{ch}^{(t)} \right) \tag{7c}$$

$$SOC^{(0)} + \Delta t \sum_{n=1}^{t} \left(\eta_{ch} p_{ch}^{(t)} - \eta_{dch} p_{dch}^{(t)} \right) \leq \overline{SOC} \tag{7d}$$

For all time $t \in \{1, \ldots, N\}$.

2.2.4. Convex model (NLP)

The Convex model (NLP), representing our proposed approach, shares identical constraints with the LP Convex model. However, it differs in its objective function, where the degradation is accounted for using the original power fit function, as presented in Eq. (8). This means that, in addition to ensuring non-simultaneous charging and discharging, our proposed model considers the impact of BESS degradation over time more accurately. The objective function is tailored to capture the non-linear relationship between BESS cycling and degradation, providing a more accurate representation of the real-world behaviour of the energy storage system. This consideration is essential for optimising the dispatch strategy while accounting for the long-term health and performance of the BESS under varying operational conditions.

$$\min_{p_{ch},p_{dch},p_{buy},p_{sell},p_{cu}} \Delta t \sum_{t=1}^{N} \left[p_{buy}^{(t)} \left(c_e^{(t)} + \varepsilon \right) - p_{sell}^{(t)} c_e^{(t)} + \mu_1 \left(\mu_2 p_{ch}^{(t)} \right)^b + \mu_1 \left(\mu_2 p_{dch}^{(t)} \right)^b \right] \tag{8}$$

Here, μ_1 is calculated as $\mu_1 = \frac{a\xi\lambda}{2}$ and is expressed in [Eur] and μ_2 is calculated as $\mu_2 = \frac{100}{\lambda}$ and is expressed in [%/MWh].

3. Model validation

To address the challenges associated with handling a large dataset for model validation, we propose the use of cluster analysis to generate scenarios for testing BESS day-ahead dispatch optimisation methods under diverse conditions. The categorisation of similar days is based on the dynamics of energy spot prices, load, and PV generation. Specifically, largest energy spot price spread (Δ_{c_e}) and balance between generated and consumed power ($\Delta_{p,max}$), are computed using the Eqs. (9a), (9b), respectively.

$$\Delta_{c_e} = max\boldsymbol{c_e} - min\boldsymbol{c_e} + \varepsilon \tag{9a}$$

$$\Delta_{p,max} = max(\Delta_p) = max\left(\boldsymbol{p_{pv}} - \boldsymbol{p_L} \right) \tag{9b}$$

The constant ε is included in calculation of Δ_{c_e} since end consumers are associated with fixed power consumption costs, which increases the minimum energy spot price difference required to pay off the full cycle of BESS. is positive in case of surplus generation and negative, in case of deficit generation. Moreover, binary features are derived from each historical day d out of the total number of historical days D, forming a feature vector $\boldsymbol{v}^d = \left[b_{c_e}^{(d)} \; b_p^{(d)} \right]$, where $b_{c_e}^{(d)}$ and $b_p^{(d)}$ are defined in Eqs. (10a), (10b), respectively.

$$b_{c_e}^{(d)} = \begin{cases} 1, if \; \Delta_{c_e}^{(d)} > \tau \\ 0, otherwise \end{cases}, \forall d \in D \tag{10a}$$

$$b_p^{(d)} = \begin{cases} 1, if \; \Delta_p^{(d)} > 0 \\ 0, otherwise \end{cases}, \forall d \in D \tag{10b}$$

Here τ represents the BESS operation costs for performing a full cycle or any maximum DoD allowed in a specific case. It acts as a threshold value for model validation, ensuring that the model(s) perform a full cycle if the energy spot price spread is larger than τ and a partial cycle or none otherwise. This feature vector can be expanded to include more energy spot price spreads specific to the market where the HRES is operating.

Since features are extracted independently from each day, this method ensures that information about the dynamics of energy spot prices and PV generation/load is not lost. After forming the feature matrix, a well-established hierarchical clustering procedure is applied using the most suitable linkage method, which is case-specific. The data normalization step can be omitted since the features are already binary. The Euclidean distance between feature vectors of any two days i and j is given by Eq. (11). The choice of Euclidean distance is common in cluster analysis for its simplicity and effectiveness in capturing the geometric relationships between feature vectors.

$$distance_{ij} = \sqrt{\left(b_{c_e}^{(i)} - b_{c_e}^{(j)} \right)^2 + \left(b_p^{(i)} - b_p^{(j)} \right)^2}, \forall i,j \in D \tag{11}$$

To evaluate and compare the performance the models, five metrics, namely, the mean absolute percentage error (MAPE), total yearly HRES savings, total yearly HRES percentage savings, BESS yearly degradation and IRR, are calculated using the hourly time step dataset of $N = 1095$ days ($M = 3$ years). MAPE is calculated with regards to actual nonlinear objective function of minimizing test case HRES daily (24 time intervals) costs, as provided in Eq. (12).

$$MAPE = \frac{100}{N} \sum_{i=1}^{1095} \left| \frac{y^{(i)} - \widehat{y}^{(i)}}{y^{(i)}} \right| \tag{12}$$

where $\widehat{y}$ represents daily optimisation objective function value of the analysed model. To calculate the total yearly HRES savings and total yearly HRES percentage savings offered by each optimisation model to the test case HRES, initially operational expenditures (OPEX) are calculated as in Eqs. (13)–(14).

$$OPEX_0 = \frac{1}{M} \sum_{i=1}^{1095} \sum_{j=1}^{24} f\left(\Delta_p^{(i,j)} \right) \tag{13}$$

$$f\left(\Delta_p^{(i,j)} \right) = \begin{cases} \Delta_p^{(i,j)} c_e^{(i,j)}, if \; \left(\Delta_p^{(i,j)} \right) > 0 \\ \Delta_p^{(i,j)} \left(c_e^{(i,j)} + \varepsilon \right), otherwise \end{cases} \tag{14}$$

Then calculate the total yearly HRES savings and total yearly HRES percentage savings can be expressed as in Eqs. (15)–(16).

$$savings = OPEX_0 - \frac{1}{M} \sum_{i=1}^{1095} \widehat{y}^{(i)} \tag{15}$$

$$savings_p = \frac{100}{OPEX_0} savings \tag{16}$$

Yearly BESS degradation (δ_{yearly}) offered by each model is calculated as in Eq. (17), where $\delta^{(i)}$ represents actual daily BESS degradation, which is evaluated using daily BESS operation dispatch optimisation results with the power fit function Eq. (5b).

$$\delta_{yearly} = \frac{1}{M} \sum_{i=1}^{1095} \delta^{(i)} \tag{17}$$

Finally, internal rate of return (IRR) is calculated as a universal financial measure that does not require assumptions on discount rate. It's an analytical solution of Eq. (18).

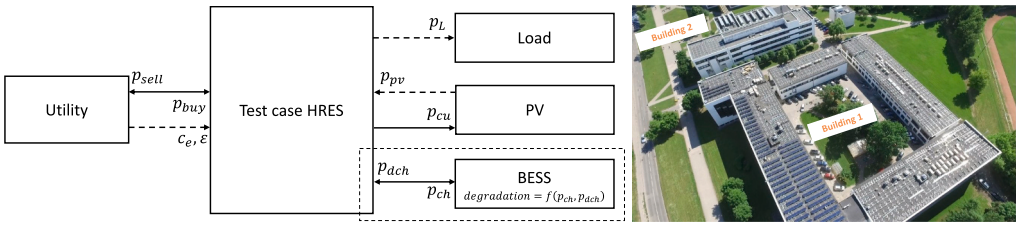

Fig. 3. a) Schematic diagram and b) photo of test case HRES.

Table 1
Test case HRES assumptions related to BESS.

Parameter	Value	Unit
ξ	150	kEur/MWh
λ	0.1	MWh
$\overline{p_{ch}}$	0.1	MW
$\overline{p_{dch}}$	0.1	MW
$SOC^{(0)}$	0.05	MWh
$\underline{SOC}$	0.005	MWh
$\overline{SOC}$	0.095	MWh
η_{ch}	90	%
η_{dch}	95	%

$$\sum_{t=0}^{T} \frac{CF^t}{(1+IRR)^t} = 0 \tag{18}$$

where CF represents yearly cash flows, considering the investment costs in BESS at $t = 0$.

4. HRES CASE study

The test case HRES is installed in Kaunas, Lithuania. It comprises two buildings with electrical load and rooftop solar PV power plants, which are aggregated and treated as a unified load and solar PV generation entity, as illustrated in Fig. 3. The rooftop PV plant comprises 20 power inverters, each equipped with 1 or 2 strings of polycrystalline PV modules, each rated at 265 W. The total installed capacity of solar PV is 380.275 kW and the total allowable power for consumption and generation is capped at 540 kW. The net consumption and PV generation amount to 1.86 GWh/year and 0.35 GWh/year, respectively.

The analysed historical period is three years (2020−2022) with the hourly time interval $\Delta t = 1$. The average energy spot price for the analysed period in the given price area is 138.08 Eur/MWh. As the test HRES is connected to the distribution network, the fixed grid usage charge for consumption ε is equal to 48.44 Eur/MWh. These energy characteristics result in an average net expenditure on energy of around 300 kEur/year.

Currently, the test case HRES does not include BESS. To perform the case study, necessary assumptions for optimisation are outlined in Table 1. The degradation costs through cycling (ξ) for Li-ion BESS fall within the range of 50 kEur/MWh to 400 kEur/MWh, as suggested by [74,75]. Therefore, we assume an intermediate value of 150 kEur/MWh. The installed capacity (λ) is constrained to 100 kWh, a relatively small capacity given the HRES size, dictated by spatial restrictions. Additionally, to extend the Li-ion BESS lifetime, tests conducted by [76] involve varying the minimum state of charge ($\underline{SOC}$) from 0 % to 15 %, and the maximum state of charge $\overline{SOC}$ from 80 % to 95 %. In line with [77], which recommends charging the BESS to 95 % SOC to prevent lithium plating, we assume $\underline{SOC}$ and $\overline{SOC}$ to range between 5 % and 95 %, respectively. Finally, typical efficiency values for Li-ion BESS charging (η_{ch}) discharging (η_{dch}), set at 90 % and 95 %, respectively, are assumed [78,79].

The historical data for energy spot prices, load, and PV generation were sourced from various databases. The energy spot prices were obtained from the market operator Nordpool, load data were provided by the distribution system operator (DSO), and PV generation data was acquired from a solar PV inverter cloud service. The gathered data were validated by checking for outliers or anomalies, which were not identified. The minimum, average and maximum values of each data parameter are given in Table 2.

Table 2
Description of validated data.

Parameter	Minimum	Average	Maximum
Price [Eur/MWh]	−56.55	138.08	4000.0
Solar PV output [kW]	0.0	39.95	328.22
Load [kW]	49.08	212.42	424.28

Fig. 4 illustrates the average dynamics of energy spot prices, PV generation, and load throughout the day. Additionally, it provides first-to-third quartile values for each hour, offering insights into potential deviations across different seasons. Notably, two significant energy spot price spreads, namely the Night-Morning Spread and Midday-Evening Spread, are observed. Furthermore, there are instances when PV generation surpasses the load during noon. This comprehensive overview aids in understanding the variations and patterns in the data over different periods as well as it suggests that two energy spot price spreads should be used in feature extraction described in the Methodology section.

4.1. Test scenarios development

In the context of the test case HRES case, we developed three model validation scenarios using cluster analysis applied to three years of historical data. The dataset involved 1095 days of energy spot price, PV generation, and load, all provided at hourly intervals. The formulation of these scenarios involved capturing the characteristic day dynamics through feature vectors $\boldsymbol{v}^d = \left[b_{c_e}^{d,0-12} \quad b_{c_e}^{d,12-24} \quad b_{p}^{d,0-24} \right]$, $d \in 1\ldots1095$. In binarization process of energy spot price spreads during the Night-Morning Spread (00:00 to 12:00) and Midday-Evening Spread (12:00 to 24:00), where threshold value $\tau = 161.14$ Eur/MWh was calculated as in Eq. (19).

$$\tau = \xi a \cdot 100^b + \varepsilon \tag{19}$$

The resulting scenarios (clusters) are visually represented in Fig. 5 and can be summarized as follows: Cluster 1 represents a situation where PV generation does not exceed the load throughout the entire day, and both energy spot price spreads are lower than τ measuring at 58.12 Eur/MWh and 55.19 Eur/MWh. In Cluster 2, PV generation also does not surpass the load for the entire day. Concerning energy spot prices, the spread between the night bottom price and morning peak price is greater than τ at 181.17 Eur/MWh, and the spread between midday bottom price and evening peak price exceeds that of scenario 1 but remains below τ measuring at 145.92 Eur/MWh. In Cluster 3, PV generation surpasses the load for 3 h during the day. Similar to scenario 1, concerning energy spot prices, both spreads are lower than τ measuring at 38.56 Eur/MWh and 51.05 Eur/MWh.

Concerning the BESS degradation costs through cycling, the optimal

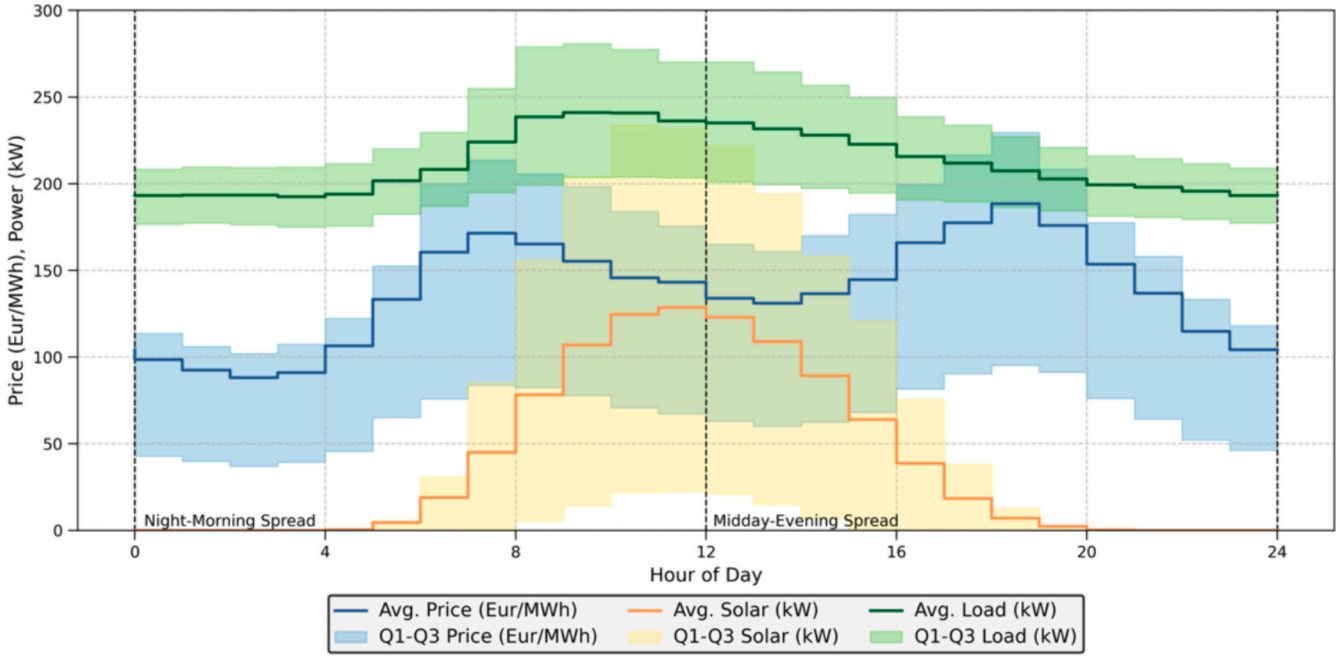

Fig. 4. Daily dynamics of energy sport price, PV generation and load.

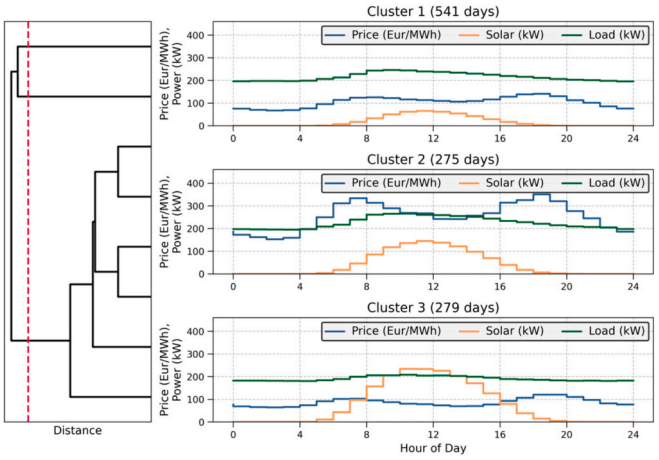

Fig. 5. Cluster analysis results (a) and corresponding representative scenarios (b).

BESS operation dispatch is expected to exhibit the following strategy: Models should suggest BESS to stay in idle mode or perform a partial cycle in scenario 1, more than one or more than one full cycle in scenario 2 (except for Naive model as there is no surplus PV generation), and again as in scenario 1, to stay in idle mode or perform a partial cycle in scenario 3. In case BESS degradation costs are disregarded (Baseline-NOD model), at least one full BESS cycle should be suggested regardless of scenario.

4.2. Model validation

The models are validated in Python 3 [80] environment. The Gurobi interface [81] is used to solve MILP problem, while the cvxpy library [82] is utilized for convex optimisation problems. Fig. 6 illustrates the model validation outcomes for scenario 1. As expected, the Naive model, as well as both the Baseline (MILP) and Convex (LP) models, recommend keeping the BESS in idle mode throughout the entire day. This suggestion is based on the observation that both energy spot price spreads fall below the threshold value τ. On the other hand, the NLP model suggests performing a partial cycle, involving charging to 76.1 % during the night and discharging during the morning and evening peak prices. This strategy results in a net HRES savings of 1.54 Eur (equivalent to 0.21 %), inclusive of BESS degradation costs (equivalent to 1.52 Eur) during the 24-hour time window from scenario 1.

In contrast, the Baseline-NOD model, which does not account for BESS degradation costs, recommends a full cycle. However, this approach leads to a net HRES loss of 5 Eur (equivalent to 0.68 %), which is caused by BESS degradation costs (equivalent to 9.91 Eur).

Fig. 7 illustrates the model validation outcomes for scenario 2. As expected, the Naive model, recommend keeping the BESS in idle mode throughout the entire day, while Baseline (MILP) and Convex (LP) models suggest performing one full cycle by charging at night and discharging in the evening. This strategy results in a net HRES savings of 3.74 Eur (equivalent to 0.28 %), inclusive of BESS degradation costs (equivalent to 9.91 Eur) during the 24-hour time window from scenario 2.

Convex (NLP) suggests not only making use of Midday-Evening price spread by performing an additional partial cycle in the middle of the day, but also perform the charging and discharging in more and smaller steps, this way exploiting the non-linear relationship between BESS degradation and DoD. This strategy results in a net HRES savings of 8.22 Eur (equivalent to 0.62 %), inclusive of BESS degradation costs (equivalent to 3.47 Eur).

Baseline-NOD (MILP) uses both spreads to perform two full cycles over the day. However, this approach leads to a net HRES loss of 2.70 Eur (equivalent to 0.20 %), which is caused by BESS degradation costs (equivalent to 19.83 Eur).

Fig. 8 illustrates the model validation outcomes for scenario 3. As expected, similarly as in scenario 1, both the Baseline (MILP) and Convex (LP) models, recommend keeping the BESS in idle mode throughout the entire day due to energy spot price spreads that fall below the threshold value τ. On the other hand, since in this scenario solar PV surplus generation occurs during the midday, Naive model strategy results in a net HRES savings of 3.74 Eur (equivalent to 0.28 %), inclusive of BESS degradation costs (equivalent to 9.91 Eur) during the 24-hour time window from scenario 3.

Convex (NLP) accounts for the smallest price spread out of all

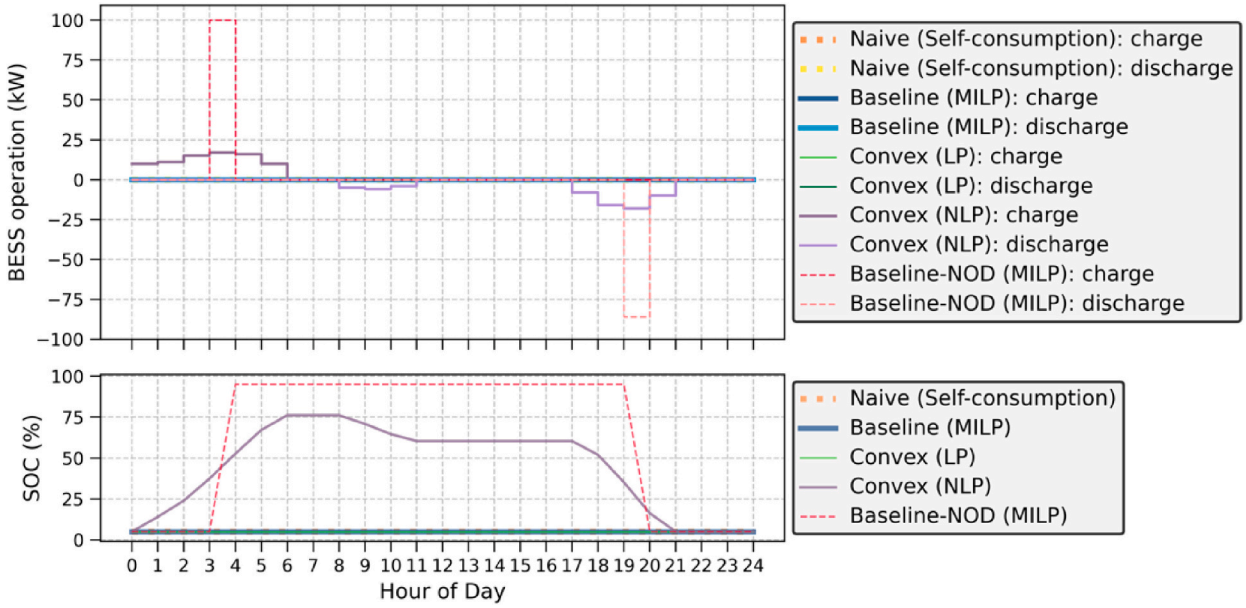

Fig. 6. Model validation using scenario 1.

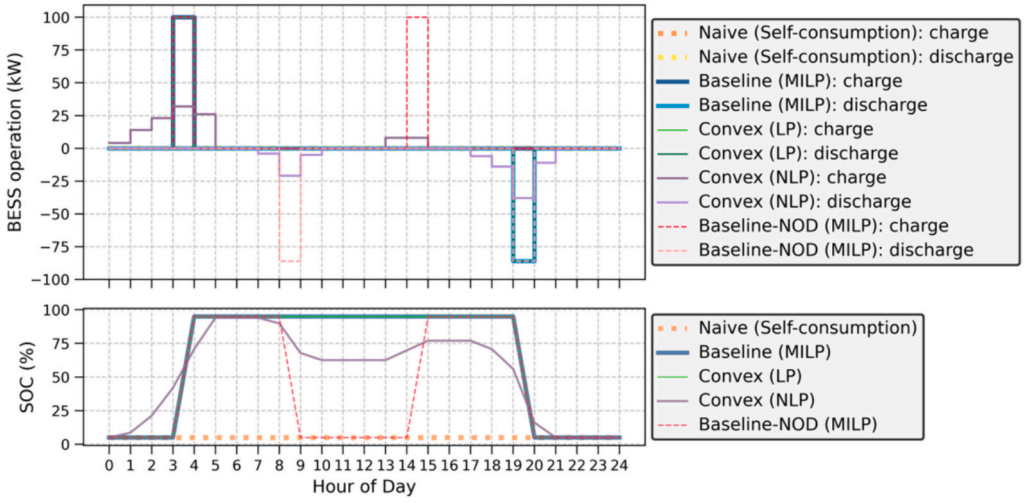

Fig. 7. Model validation using scenario 2.

validation scenarios and suggests performing only two partial cycles. Although Night-Morning Spread is larger than the Midday-Evening Spread, the BESS performs a larger partial cycle during the second half of the day due to surplus energy accumulated during the midday. This strategy results in a net HRES savings of 2.63 Eur (equivalent to 0.69 %), inclusive of BESS degradation costs (equivalent to 2.36 Eur).

Baseline-NOD (MILP) uses both spreads and surplus solar PV generation to perform two full cycles over the day. However, this approach leads to a net HRES loss of 8.52 Eur (equivalent to 2.23 %), which is caused by BESS degradation costs (equivalent to 16.03 Eur).

4.3. Overall results

After the model performance is validated, the optimisation models are applied to the whole three years dataset and generalized metrics are calculated and provided in Table 3. Starting with the Naive (Self-consumption) model, it demonstrates a Mean Absolute Percentage Error (MAPE) of 0.87 %, indicating that it is a relatively accurate model. The corresponding net savings for the HRES amount to 0.90 % per year, with costs and BESS degradation at 0.15 % and 3.00 % per year, respectively. The Internal Rate of Return (IRR) for this model is recorded at 12.18 %. Such low IRR value is the result of BESS being charged solely during periods of surplus PV generation, leading to an average of only 0.234 cycles per day.

The Baseline (MILP) and Convex (LP) models, both exhibit similar MAPE values of 0.65 %, suggesting comparable optimisation accuracy. The net savings for the HRES are 1.54 % and 1.55 % per year for the MILP and LP models, respectively. Costs for both models hover around 0.54 %, while BESS degradation is more pronounced in the MILP model at 10.67 %, compared to the LP model at 10.52 %. The IRR for these models is notably higher, reaching 28.10 % and 28.29 %, respectively. This is caused by the increased engagement of BESS, resulting in an average of 0.47 cycles per day.

In contrast, the Convex (NLP) model outperforms all other models with a perfect MAPE of 0 %. Since, this model by nature prefers partial cycling, it makes 1.1 cycle per day on average, leading to the highest net savings among analysed models, standing at 1.99 % per year, with costs and BESS degradation at 0.44 % and 8.77 % per year, respectively.

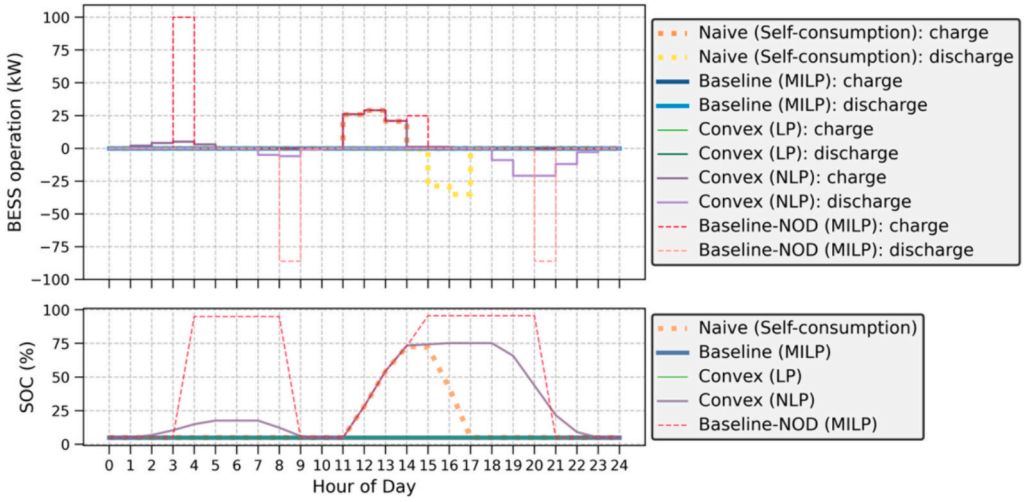

Fig. 8. Model validation using scenario 3.

Table 3
Summary of model performance comparison.

Optimisation model	MAPE [%]	BESS cycles [cycles/day]	HRES net savings [%/year]	HRES costs [%/year]	BESS degradation [%/year]	IRR [%]
Naive (self-consumption)	0.87	0.23	0.90	0.15	3.00	12.18
Baseline (MILP)	0.65	0.47	1.54	0.54	10.67	28.10
Convex (LP)	0.65	0.47	1.55	0.53	10.52	28.29
Convex (NLP)	0	1.1	1.99	0.44	8.77	38.03
Baseline-NOD (MILP)	1.07	1.96	0.55	2.27	45.17	1.68

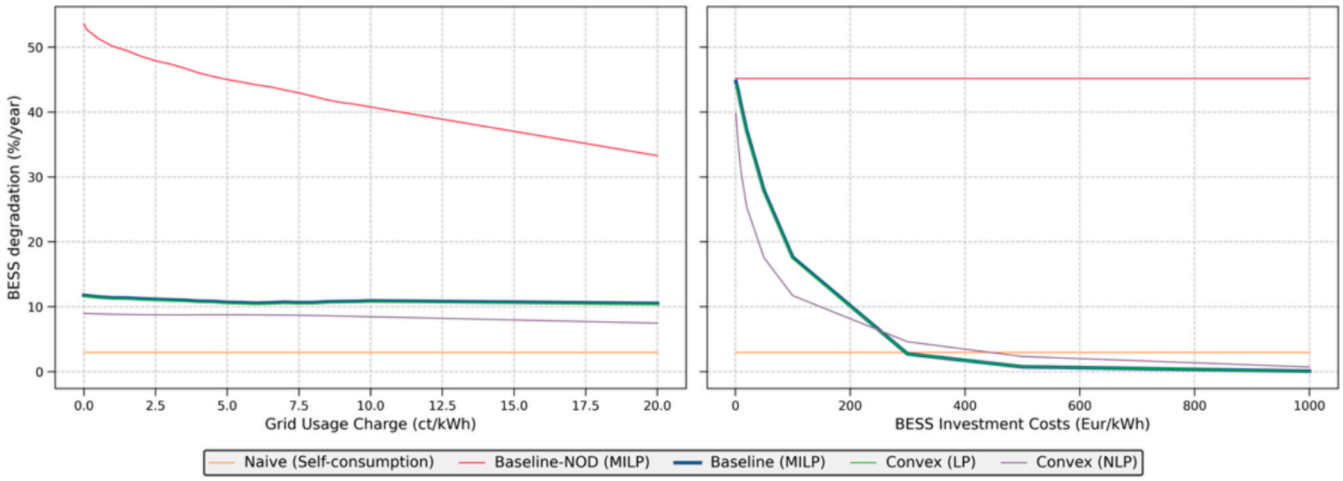

Fig. 9. BESS degradation sensitivity analysis.

Consequently, the IRR for the Convex (NLP) model is also the most substantial, reaching 38.03 %.

Lastly, the Baseline-NOD (MILP) model, which disregards BESS degradation costs, exhibits MAPE of 1.07 %. The net savings are lower than the proposed model at 0.55 % per year, while costs increase significantly to 2.27 %. Due to the fact that this model allows almost 2 cycles per day, the BESS degradation, is remarkably high at 45.17 % per year, which results in the lowest IRR of all models, equal to 1.68 %. This highlights the importance of considering degradation costs in the overall economic analysis of the HRES.

4.4. Sensitivity analysis

The sensitivity analysis of BESS degradation to parameters ε (the fixed grid usage charge) and ξ (BESS investment costs) is depicted in Fig. 9. The examination reveals that the implementation of either LP or NLP BESS operation dispatch optimisation methods in HRES influences BESS degradation in a linear relationship as ε increases. This linear relationship can be explained by the nature of ε, which can be considered a component that increased the energy spot price spread at which BESS cycling is profitable. Consequently, the larger the price spread required for cycling, the fewer cycles are executed per year, resulting in reduced BESS degradation.

In contrast to the linear relationship, degradation demonstrates an exponential decrease as ξ increases, leading to minimal BESS exploitation when investment costs surpass 500 Eur/kWh. In comparison to linear models, our proposed method is dominant, as it utilizes partial cycling and enables increased BESS degradation, especially, if ξ exceeds

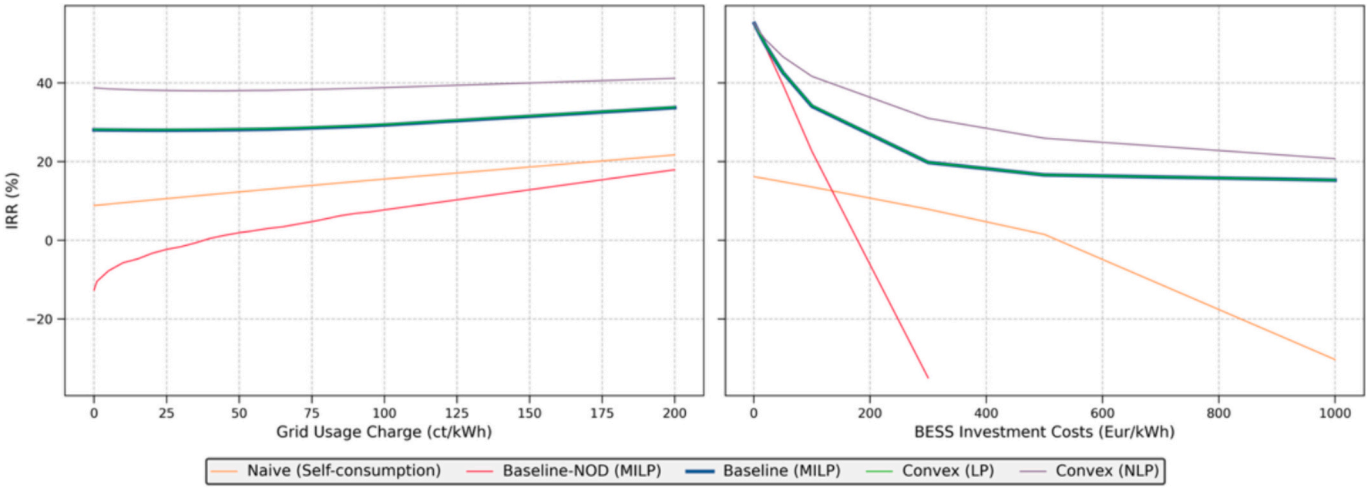

Fig. 10. IRR sensitivity analysis.

250 Eur/MWh. This approach allows for a more flexible and adaptive management of BESS in response to varying investment costs, offering a more tailored solution for HRES.

The sensitivity analysis of BESS IRR to parameters ε and ξ is depicted in Fig. 10. In negative correlation to previous sensitivity analysis results, as ε increases, the IRR also increases. This can be explained by the fact, that as ε increases, the total test case HRES costs related to purchased power also increases and, thus, since BESS is degraded less, the costs associated with it also decreases and the net savings per year increases, resulting in increasing IRR. Naturally, as the ξ increases, IRR decreases exponentially. Once again, implementation of our proposed method allows increasing the IRR of HRES.

The sensitivity analysis of BESS IRR to parameters ε and ξ is illustrated in Fig. 10. In contrast to the previous sensitivity analysis results, there is a negative correlation between ε and IRR. As ε increases, the IRR also increases. This can be explained by the fact that as ε increases, the total HRES costs related to purchased power also increase. Consequently, since BESS is degraded less, the costs associated with it decrease, leading to an increase in net savings per year and, ultimately, an increase in IRR.

5. Conclusions

Involvement of degradation costs into BESS operation dispatch optimisation problem is crucial. Without this consideration, total HRES operational costs could increase, potentially leading to non-profitable investment in BESS. Baseline (MILP) and Convex (LP) models yielded identical results, confirming that convexity rules can effectively address BESS dispatch optimisation problem. Our proposed Convex (NLP) model, in contrast to other commonly used models, accurately accounts for BESS degradation, resulting in more frequent activation of BESS at partial cycling. This is significant because partial cycling tends to degrade BESS at a slower rate than full cycling due to the nonlinear relationship between BESS degradation and DoD.

Exploiting this phenomenon, the Convex NLP model can adapt to a wide spectrum of daily energy spot prices, solar PV generation, and load dynamics scenarios. As a result, the application of our model in economic feasibility studies enables a more precise evaluation of the expected BESS return. The integration of the proposed algorithm into the energy management system demonstrates a significant increase in the number of BESS cycles, specifically 2.36 times more compared to commonly used MILP and LP models. Consequently, integrating such an algorithm into the HRES energy management system could lead to an increased IRR value of the project by up to 10 %, as evidenced in our case study. Furthermore, as the BESS state of health decreases over the years, more cycles are performed annually, resulting in higher energy throughput of BESS over its lifetime.

The capabilities of the proposed method will be further investigated in more complex applications, such as stochastic optimisation and optimal sizing of BESS. Additionally, the convexity feature presents opportunities for testing Machine Learning applications. This includes utilizing optimisation with forecasts and enhancing computational speed, addressing potential challenges in larger-scale applications. Finally, to further enhance the model accuracy, we will explore the convexity of the BESS degradation function, incorporating additional important parameters, such as temperature and C-rate.

CRediT authorship contribution statement

Jonas Vaičys: Writing – review & editing, Writing – original draft, Methodology, Investigation, Data curation, Conceptualization. **Saulius Gudžius:** Writing – review & editing, Visualization, Supervision, Investigation, Data curation, Conceptualization. **Audrius Jonaitis:** Resources, Funding acquisition, Data curation. **Roma Račkienė:** Data curation, Writing – review & editing, Resources. **Andrei Blinov:** Writing – review & editing, Formal analysis. **Dimosthenis Peftitsis:** Writing – review & editing, Formal analysis.

Declaration of competing interest

The authors declare that they have no known competing financial interests or personal relationships that could have appeared to influence the work reported in this paper.

Data availability

Data will be made available on request.

Acknowledgements

This research was supported by the European Economic Area (EEA) and Norway Financial Mechanism 2014–2021 under Grant EMP474 and by Research Council of Lithuania (LMTLT), agreement No S-A-UEI-23-1 (22-12-2023).

References

[1] Q. Hassan, S. Algburi, A.Z. Sameen, T.J. Al-Musawi, A.K. Al-Jiboory, H.M. Salman, B.M. Ali, M. Jaszczur, A comprehensive review of international renewable energy growth, Energy Built Environ. (2024), https://doi.org/10.1016/j.enbenv.2023.12.002.

[2] J. Chen, S. Huang, H.W. Kamran, Empowering sustainability practices through energy transition for sustainable development goal 7: the role of energy patents and natural resources among European Union economies through advanced panel, Energy Policy 176 (2023) 113499, https://doi.org/10.1016/j.enpol.2023.113499.
[3] J. He, Y. Yang, Z. Liao, A. Xu, K. Fang, Linking SDG 7 to assess the renewable energy footprint of nations by 2030, Appl. Energy 317 (2022) 119167, https://doi.org/10.1016/j. apenergy.2022.119167.
[4] COP28 Presidency, IRENA and GRA, Tripling Renewable Power and Doubling Energy Efficiency by 2030. https://www.irena.org/Publications/2023/Oct/Tripling-renewable-power-and-doubling-energy-efficiency-by-2030, 2023.
[5] S. Islam, N.K. Roy, Renewables integration into power systems through intelligent techniques: implementation procedures, key features, and performance evaluation, Energy Rep. 9 (2023) 6063–6087, https://doi.org/10.1016/j.egyr.2023.05.063.
[6] M. Amir, R.G. Deshmukh, H.M. Khalid, Z. Said, A. Raza, S.M. Muyeen, A.-S. Nizami, R.M. Elavarasan, R. Saidur, K. Sopian, Energy storage technologies: an integrated survey of developments, global economical/environmental effects, optimal scheduling model, and sustainable adaption policies, J. Energy Storage 72 (2023) 108694, https://doi.org/10.1016/j.est.2023.108694.
[7] M. Aneke, M. Wang, Energy storage technologies and real life applications – a state of the art review, Appl. Energy 179 (2016) 350–377, https://doi.org/10.1016/j.apenergy.2016.06.097.
[8] T.M.I. Mahlia, T.J. Saktisahdan, A. Jannifar, M.H. Hasan, H.S.C. Matseelar, A review of available methods and development on energy storage; technology update, Renew. Sustain. Energy Rev. 33 (2014) 532–545, https://doi.org/10.1016/j.rser.2014.01.068.
[9] S. Barbhuiya, B.B. Das, M. Idrees, Thermal energy storage in concrete: a comprehensive review on fundamentals, technology and sustainability, J. Build. Eng. 82 (2024) 108302, https://doi.org/10.1016/j.jobe.2023.108302.
[10] E. Wenger, M. Epstein, A. Kribus, Thermo-electro-chemical storage (TECS) of solar energy, Appl. Energy 190 (2017) 788–799, https://doi.org/10.1016/j.apenergy.2017.01.014.
[11] A. Jonaitis, S. Gudzius, A. Morkvenas, M. Azubalis, I. Konstantinaviciute, A. Baranauskas, V. Ticka, Challenges of integrating wind power plants into the electric power system: Lithuanian case, Renew. Sustain. Energy Rev. 94 (2018) 468–475, https://doi.org/10.1016/j.rser.2018.06.032.
[12] O.S. Burheim, Mechanical energy storage, Eng. Energy Storage (2017) 29–46, https://doi.org/10.1016/b978-0-12-814100-7.00003-1.
[13] H. Ibrahim, A. Ilinca, J. Perron, Energy storage systems—characteristics and comparisons, Renew. Sustain. Energy Rev. 12 (2008) 1221–1250, https://doi.org/10.1016/j.rser.2007.01.023.
[14] M.M. Rana, M. Uddin, M.R. Sarkar, S.T. Meraj, G.M. Shafiullah, S.M. Muyeen, Md. A. Islam, T. Jamal, Applications of energy storage systems in power grids with and without renewable energy integration — a comprehensive review, J. Energy Storage 68 (2023) 107811, https://doi.org/10.1016/j.est.2023.107811.
[15] F.S.M. Mviri, Battery storage systems in electric power grid: a review, J. Phys. Conf. Ser. 2276 (2022) 012016, https://doi.org/10.1088/1742-6596/2276/1/012016.
[16] D.O. Akinyele, R.K. Rayudu, Review of energy storage technologies for sustainable power networks, Sustain Energy Technol Assess 8 (2014) 74–91, https://doi.org/10.1016/j.seta.2014.07.004.
[17] C.A. Moreno-Camacho, J.R. Montoya-Torres, A. Jaegler, N. Gondran, Sustainability metrics for real case applications of the supply chain network design problem: a systematic literature review, J. Clean. Prod. 231 (2019) 600–618, https://doi.org/10.1016/j.jclepro.2019.05.278.
[18] A. Castillo, D.F. Gayme, Grid-scale energy storage applications in renewable energy integration: a survey, Energ. Conver. Manage. 87 (2014) 885–894, https://doi.org/10.1016/j.enconman.2014.07.063.
[19] M. Skyllas-Kazacos, Electro-chemical energy storage technologies for wind energy systems, in: Stand-Alone and Hybrid Wind Energy Systems, 2010, pp. 323–365, https://doi.org/10.1533/9781845699628.2.323.
[20] K.C. Divya, J. Østergaard, Battery energy storage technology for power systems—an overview, Electr. Pow. Syst. Res. 79 (2009) 511–520, https://doi.org/10.1016/j.epsr.2008.09.017.
[21] M. Ghiji, V. Novozhilov, K. Moinuddin, P. Joseph, I. Burch, B. Suendermann, G. Gamble, A review of lithium-ion battery fire suppression, Energies 13 (2020) 5117, https://doi.org/10.3390/en13195117.
[22] M.D. Bhatt, J.Y. Lee, High capacity conversion anodes in Li-ion batteries: a review, Int. J. Hydrogen Energy 44 (2019) 10852–10905, https://doi.org/10.1016/j.ijhydene.2019.02.015.
[23] K. Li, K.J. Tseng, Energy efficiency of lithium-ion battery used as energy storage devices in micro-grid, in: IECON 2015-41st Annual Conference of the IEEE Industrial Electronics Society, 2015, https://doi.org/10.1109/iecon.2015.7392923.
[24] H. Shan, H. Cao, X. Xu, T. Xiao, G. Hou, H. Cao, Y. Tang, G. Zheng, Investigation of self-discharge properties and a new concept of open-circuit voltage drop rate in lithium-ion batteries, J. Solid State Electrochem. 26 (2021) 163–170, https://doi.org/10.1007/s10008-021-05049-y.
[25] T. Takamura, M. Uehara, J. Suzuki, K. Sekine, K. Tamura, High capacity and long cycle life silicon anode for Li-ion battery, J. Power Sources 158 (2006) 1401–1404, https://doi.org/10.1016/j.jpowsour.2005.10.081.
[26] D.D. Agwu, F.K. Opara, N. Chukwuchekwa, D.O. Dike, L. Uzoechi, Review of Comparative Battery Energy Storage Systems (BESS) for Energy Storage Applications in Tropical Environments, 2017 IEEE 3rd International Conference on Electro-Technology for National Development (NIGERCON), 2017.
[27] Z. Song, K. Feng, H. Zhang, P. Guo, L. Jiang, Q. Wang, H. Zhang, X. Li, "Giving comes before receiving": high performance wide temperature range Li-ion battery with Li5V2(PO4)3 as both cathode material and extra Li donor, Nano Energy 66 (2019) 104175, https://doi.org/10.1016/j.nanoen.2019.104175.
[28] S. Mulder, S. Klein, Techno-economic comparison of electricity storage options in a fully renewable energy system, Energies 17 (2024) 1084, https://doi.org/10.3390/en17051084.
[29] H. Hesse, M. Schimpe, D. Kucevic, A. Jossen, Lithium-ion battery storage for the grid—a review of stationary battery storage system design tailored for applications in modern power grids, Energies 10 (2017) 2107, https://doi.org/10.3390/en10122107.
[30] D. Choi, N. Shamim, A. Crawford, Q. Huang, C.K. Vartanian, V.V. Viswanathan, M. D. Paiss, M.J.E. Alam, D.M. Reed, V.L. Sprenkle, Li-ion battery technology for grid application, J. Power Sources 511 (2021) 230419, https://doi.org/10.1016/j.jpowsour.2021.230419.
[31] G. Wang, M. Ciobotaru, V.G. Agelidis, Optimal capacity design for hybrid energy storage system supporting dispatch of large-scale photovoltaic power plant, J. Energy Storage 3 (2015) 25–35, https://doi.org/10.1016/j.est.2015.08.006.
[32] C.S. Makola, P.F. Le Roux, J.A. Jordaan, Comparative analysis of lithium-ion and lead–acid as electrical energy storage systems in a grid-tied microgrid application, Appl. Sci. 13 (2023) 3137, https://doi.org/10.3390/app13053137.
[33] T. Bocklisch, Hybrid energy storage approach for renewable energy applications, J. Energy Storage 8 (2016) 311–319, https://doi.org/10.1016/j.est.2016.01.004.
[34] O.E. Olabode, T.O. Ajewole, I.K. Okakwu, A.S. Alayande, D.O. Akinyele, Hybrid power systems for off-grid locations: a comprehensive review of design technologies, applications and future trends, Scientific African. 13 (2021) e00884, https://doi.org/10.1016/j. sciaf.2021.e00884.
[35] S. Goel, R. Sharma, Performance evaluation of stand alone, grid connected and hybrid renewable energy systems for rural application: a comparative review, Renew. Sustain. Energy Rev. 78 (2017) 1378–1389, https://doi.org/10.1016/j.rser.2017.05.200.
[36] J. Vaicys, P. Norkevicius, A. Baronas, S. Gudzius, A. Jonaitis, D. Peftitsis, Efficiency evaluation of the dual system power inverter for on-grid photovoltaic system, Energies 15 (2021) 161, https://doi.org/10.3390/en15010161.
[37] B. Adebanji, O. Atoki, T. Fasina, O. Adetan, A. Abe, Comparative study of off-grid and grid-connected hybrid power system: issues, future prospects and policy framework, IJEECS 22 (2021) 752, https://doi.org/10.11591/ijeecs.v22.i2.pp752-759.
[38] V. Karthikeyan, S. Rajasekar, V. Das, P. Karuppanan, A.K. Singh, Grid-connected and off-grid solar photovoltaic system, Smart Energy Grid Design for Island Countries. (2017) 125–157, https://doi.org/10.1007/978-3-319-50197-0_5.
[39] J.M. Tabora, U.C. Paixão Júnior, C.E.M. Rodrigues, U.H. Bezerra, M.E. de L. Tostes, B.S. de Albuquerque, E.O. de Matos, A.A. do Nascimento, Hybrid system assessment in on-grid and off-grid conditions: a technical and economical approach, Energies 14 (2021) 5284, https://doi.org/10.3390/en14175284.
[40] K. Basaran, N.S. Cetin, S. Borekci, Energy management for on-grid and off-grid wind/PV and battery hybrid systems, IET Renew. Power Gen. 11 (2017) 642–649, https://doi.org/10.1049/iet-rpg.2016.0545.
[41] M. Naderi, D. Palmer, M.J. Smith, E.E.F. Ballantyne, D.A. Stone, M.P. Foster, D. T. Gladwin, A. Khazali, Y. Al-Wreikat, A. Cruden, et al., Techno-economic planning of a fully renewable energy-based autonomous microgrid with both single and hybrid energy storage systems, Energies 17 (2024) 788, https://doi.org/10.3390/en17040788.
[42] T. Adefarati, R.C. Bansal, T. Shongwe, R. Naidoo, M. Bettayeb, A.K. Onaolapo, Optimal energy management, technical, economic, social, political and environmental benefit analysis of a grid-connected PV/WT/FC hybrid energy system, Energ. Conver. Manage. 292 (2023) 117390, https://doi.org/10.1016/j.enconman.2023.117390.
[43] S. Twaha, M.A.M. Ramli, A review of optimization approaches for hybrid distributed energy generation systems: off-grid and grid-connected systems, Sustain. Cities Soc. 41 (2018) 320–331, https://doi.org/10.1016/j.scs.2018.05.027.
[44] A. Etxeberria, I. Vechiu, H. Camblong, J.M. Vinassa, Hybrid Energy Storage Systems for Renewable Energy Sources Integration in Microgrids: A Review, 2010 Conference Proceedings IPEC, 2010, https://doi.org/10.1109/ipecon.2010.5697053.
[45] A. Bharatee, P.K. Ray, A. Ghosh, Power distribution technique and small-signal modeling of grid-integrated solar PV system with hybrid energy storage systems, J. Energy Storage 73 (2023) 109316, https://doi.org/10.1016/j.est.2023.109316.
[46] S. Weitemeyer, D. Kleinhans, T. Vogt, C. Agert, Integration of renewable energy sources in future power systems: the role of storage, Renew. Energy 75 (2015) 14–20, https://doi.org/10.1016/j.renene.2014.09.028.
[47] S. Günther, A. Bensmann, R. Hanke-Rauschenbach, Theoretical dimensioning and sizing limits of hybrid energy storage systems, Appl. Energy 210 (2018) 127–137, https://doi.org/10.1016/j.apenergy.2017.10.116.
[48] J. Zhang, J. Liu, L. Chen, L. Zhang, P. Zeng, Y. Li, Reliability evaluation of high permeability renewable energy distribution network considering energy storage charge and discharge strategy, Energy Rep. 9 (2023) 361–368, https://doi.org/10.1016/j.egyr.2023.01.006.
[49] T. Zimmermann, P. Keil, M. Hofmann, M.F. Horsche, S. Pichlmaier, A. Jossen, Review of system topologies for hybrid electrical energy storage systems, J. Energy Storage 8 (2016) 78–90, https://doi.org/10.1016/j.est.2016.09.006.
[50] A.F. Ramos, I. Ahmad, D. Habibi, T.S. Mahmoud, Placement and sizing of utility-size battery energy storage systems to improve the stability of weak grids, Int. J. Electrical Power & Energy Syst. 144 (2023) 108427, https://doi.org/10.1016/j.ijepes.2022.108427.
[51] A.M. Abdelshafy, J. Jurasz, H. Hassan, A.M. Mohamed, Optimized energy management strategy for grid connected double storage (pumped storage-battery)

system powered by renewable energy resources, Energy 192 (2020) 116615, https://doi.org/10.1016/j.energy.2019.116615.
[52] R.A. Ufa, V.E. Rudnik, Y.Y. Malkova, Y.D. Bay, N.M. Kosmynina, Impact of renewable generation unit on stability of power systems, Int. J. Hydrogen Energy 47 (2022) 19947–19954, https://doi.org/10.1016/j.ijhydene.2022.04.141.
[53] S.C. Johnson, D.J. Papageorgiou, M.R. Harper, J.D. Rhodes, K. Hanson, M. E. Webber, The economic and reliability impacts of grid-scale storage in a high penetration renewable energy system, Adv. Appl. Energy 3 (2021) 100052, https://doi.org/10.1016/j.adapen.2021.100052.
[54] M. Zhang, W. Li, S.S. Yu, K. Wen, S.M. Muyeen, Day-ahead optimization dispatch strategy for large-scale battery energy storage considering multiple regulation and prediction failures, Energy 270 (2023) 126945, https://doi.org/10.1016/j.energy.2023.126945.
[55] T.V. Kumar, M. Mathankumar, A. Manjunathan, J. Sathyaraj, Time based costing of energy storage system with optimal scheduling and dispatch under demand, Mater. Today: Proc. 45 (2021) 1738–1741, https://doi.org/10.1016/j.matpr.2020.08.620.
[56] M. Lee, J. Park, S.-I. Na, H.S. Choi, B.-S. Bu, J. Kim, An analysis of battery degradation in the integrated energy storage system with solar photovoltaic generation, Electronics 9 (2020) 701, https://doi.org/10.3390/electronics9040701.
[57] N. Shamarova, K. Suslov, P. Ilyushin, I. Shushpanov, Review of battery energy storage systems modeling in microgrids with renewables considering battery degradation, Energies 15 (2022) 6967, https://doi.org/10.3390/en15196967.
[58] V.S. Diaz, D.A. Cantane, A.Q.O. Santos, O.H. Ando Junior, Comparative analysis of degradation assessment of battery energy storage systems in PV smoothing application, Energies 14 (2021) 3600, https://doi.org/10.3390/en14123600.
[59] I. González, A.J. Calderón, F.J. Folgado, IoT real time system for monitoring lithium-ion battery long-term operation in microgrids, J. Energy Storage 51 (2022) 104596, https://doi.org/10.1016/j.est.2022.104596.
[60] K. Garifi, K. Baker, D. Christensen, B. Touri, Non-Simultaneous Charging and Discharging Guarantees in Energy Storage System Models for Home Energy Management Systems, 2018.
[61] D. Cremoncini, G.F. Frate, A. Bischi, L. Ferrari, Mixed Integer Linear Program Model for Optimized Scheduling of a Vanadium Redox Flow Battery with Variable Efficiencies, Capacity Fade, and Electrolyte Maintenance, 2022.
[62] C.N. Dimitriadis, E.G. Tsimopoulos, M.C. Georgiadis, Optimization-based economic analysis of energy storage technologies in a coupled electricity and natural gas market, J. Energy Storage 58 (2023) 106332, https://doi.org/10.1016/j.est.2022.106332.
[63] Y. Shen, W. Hu, M. Liu, F. Yang, X. Kong, Energy storage optimization method for microgrid considering multi-energy coupling demand response, J. Energy Storage 45 (2022) 103521, https://doi.org/10.1016/j.est.2021.103521.
[64] S. Burer, A.N. Letchford, Non-convex mixed-integer nonlinear programming: a survey, Surveys in Operations Research and Management Science. 17 (2012) 97–106, https://doi.org/10.1016/j.sorms.2012.08.001.
[65] Y. Li, X. Tang, X. Lin, L. Grzesiak, X. Hu, The role and application of convex modeling and optimization in electrified vehicles, Renew. Sustain. Energy Rev. 153 (2022) 111796, https://doi.org/10.1016/j.rser.2021.111796.
[66] P. Bonami, L.T. Biegler, A.R. Conn, G. Cornuéjols, I.E. Grossmann, C.D. Laird, J. Lee, A. Lodi, F. Margot, N. Sawaya, A. Wächter, An algorithmic framework for convex mixed integer nonlinear programs, Discret. Optim. 5 (2008) 186–204, https://doi.org/10.1016/j.disopt.2006.10.011.
[67] A. Joshi, H. Kebriaei, V. Mariani, L. Glielmo, A Sufficient Condition to Guarantee Non-Simultaneous Charging and Discharging of Household Battery Energy Storage, 2021.
[68] K. Garifi, K. Baker, D. Christensen, B. Touri, Convex relaxation of grid-connected energy storage system models with complementarity constraints in DC OPF, IEEE Trans. Smart Grid. 11 (2020) 4070–4079, https://doi.org/10.1109/tsg.2020.2987785.
[69] R. Anand, D. Aggarwal, V. Kumar, A comparative analysis of optimization solvers, J. Stat. Manag. Syst. 20 (2017) 623–635, https://doi.org/10.1080/09720510.2017.1395182.
[70] S.H. Kim, Y.-J. Shin, Optimize the operating range for improving the cycle life of battery energy storage systems under uncertainty by managing the depth of discharge, J. Energy Storage 73 (2023) 109144, https://doi.org/10.1016/j.est.2023.109144.
[71] J. Urquizo, P. Singh, Partial cycling aging of Li-ion batteries in frequency regulation applications, J. Power Sources 592 (2024) 233908, https://doi.org/10.1016/j.jpowsour.2023.233908.
[72] D. Dallinger, J. Link, M. Buttner, Smart Grid Agent: Plug-in Electric Vehicle, Working Papers "Sustainability and Innovation" S8/2013, Fraunhofer Institute for Systems and Innovation Research (ISI), 2013.
[73] A.O. Ali, A.M. Hamed, M.M. Abdelsalam, M.N. Sabry, M.R. Elmarghany, Energy manage- ment of photovoltaic-battery system connected with the grid, J. Energy Storage 55 (2022) 105865, https://doi.org/10.1016/j.est.2022.105865.
[74] J.-O. Lee, Y.-S. Kim, Novel battery degradation cost formulation for optimal scheduling of battery energy storage systems, Int. J. Electrical Power & Energy Syst. 137 (2022) 107795, https://doi.org/10.1016/j.ijepes.2021.107795.
[75] S. Few, O. Schmidt, G.J. Offer, N. Brandon, J. Nelson, A. Gambhir, Prospective improve- ments in cost and cycle life of off-grid lithium-ion battery packs: an analysis informed by expert elicitations, Energy Policy 114 (2018) 578–590, https://doi.org/10.1016/j.enpol.2017.12.033.
[76] K. Uddin, T. Jackson, W.D. Widanage, G. Chouchelamane, P.A. Jennings, J. Marco, On the possibility of extending the lifetime of lithium-ion batteries through optimal V2G facilitated by an integrated vehicle and smart-grid system, Energy 133 (2017) 710–722, https://doi.org/10.1016/j.energy.2017.04.116.
[77] H. Ruan, B. Sun, J. Jiang, X. Su, X. He, S. Ma, W. Gao, Optimal switching temperature for multi-objective heated-charging of lithium-ion batteries at subzero temperatures, J. Power Sources 562 (2023) 232775, https://doi.org/10.1016/j.jpowsour.2023.232775.
[78] X. Su, B. Sun, J. Wang, H. Ruan, W. Zhang, Y. Bao, Experimental study on charging energy efficiency of lithium-ion battery under different charging stress, J. Energy Storage 68 (2023) 107793, https://doi.org/10.1016/j.est.2023.107793.
[79] J. Elio, M. Peinado-Guerrero, R. Villalobos, R.J. Milcarek, An energy storage dispatch optimization for demand-side management in industrial facilities, J. Energy Storage 53 (2022) 105063, https://doi.org/10.1016/j.est.2022.105063.
[80] G. Van Rossum, F.L. Drake, Python 3 Reference Manual, Scotts Valley, CA, CreateSpace, 2009. https://www.python.org.
[81] Gurobi Optimization, LLC, Gurobi Optimizer Reference Manual. https://www.gurobi.com, 2023.
[82] S. Diamond, S. Boyd, A python-embedded modeling language for convex optimization, J. Mach. Learn. Res. 17 (2016) 1–5.